

Physiologically Based Pharmacokinetic (PBPK) Modeling of Pitavastatin and Atorvastatin to Predict Drug-Drug Interactions (DDIs)

Peng Duan^{1,3} · Ping Zhao² · Lei Zhang²

Published online: 17 November 2016
© Springer-Verlag Berlin Heidelberg (Outside the USA) 2016

Abstract

Background The disposition of statins varies and involves both metabolizing enzymes and transporters, making predictions of statin drug-drug interactions (DDIs) challenging. Physiologically based pharmacokinetic (PBPK) models have, however, demonstrated ability to predict complex DDIs.

Objective In this study, PBPK models of two statins (pitavastatin and atorvastatin) were developed and applied to predict pitavastatin and atorvastatin associated DDIs.

Method Pitavastatin and atorvastatin PBPK models were developed using in vitro and human pharmacokinetic data in a population-based PBPK software (SimCYP[®]) by considering the contribution of both metabolizing enzymes and transporters to their overall pharmacokinetics. The statin PBPK models and software's built-in or published models of inhibitors were used to predict DDIs under different scenarios.

Results The statin models reasonably predicted the observed exposure change due to Organic Anion Transporting Polypeptide (OATP) 1B1 polymorphism or clinical DDIs with itraconazole, erythromycin, and gemfibrozil, while under-predicted the observed DDIs caused by rifampin and cyclosporine. Further analysis demonstrated that OATP1B1 inhibition by rifampin or cyclosporine in the existing inhibitor models needs to be approximately tenfold stronger to recapitulate the observed DDI with these two inhibitors.

Conclusion Through quantitative assessment of the effect of OATP1B1 genetic polymorphism and inhibitors of transporters and metabolizing enzymes via PBPK modeling, we confirmed the importance of OATP1B1 in the disposition of these two statins, and explored potential causes for under-prediction of the inhibitory effect of rifampin and cyclosporine.

Part of this manuscript was presented as a poster at the 2015 American Society for Clinical Pharmacology and Therapeutics (ASCPT) Annual Meeting in New Orleans, LA.

The opinions in this paper are those of authors and do not necessarily reflect the official views of the FDA.

Electronic supplementary material The online version of this article (doi:10.1007/s13318-016-0383-9) contains supplementary material, which is available to authorized users.

✉ Lei Zhang
leik.zhang@fda.hhs.gov

¹ Office of Commissioner, USFDA, Silver Spring, MD, USA

² Office of Clinical Pharmacology, Office of Translational Sciences, Center for Drug Evaluation and Research, USFDA, Silver Spring, MD 20993, USA

³ Present Address: Office of New Drug Products, Office of Pharmaceutical Quality, Center for Drug Evaluation and Research, USFDA, Silver Spring, MD, USA

Key Points

Pitavastatin and atorvastatin PBPK models were successfully developed by considering the contribution of both metabolizing enzymes and transporters to their overall pharmacokinetics. The statin PBPK models reasonably predicted the observed exposure change due to OATP1B1 polymorphism or clinical DDIs with Cytochrome P450 (CYP) inhibitors or OATP1B1 inhibitors.

Further analysis demonstrated that OATP1B1 inhibition by rifampin or cyclosporine in the existing inhibitor models needs to be approximately tenfold stronger to recapitulate the observed DDI with these two inhibitors.

K_i values of inhibitor drugs on OATP1B1 need to be carefully evaluated with known substrates for a comprehensive DDI risk assessment to avoid possible under-prediction of clinical DDI.

1 Introduction

Statins are a class of drugs prescribed widely among 20 million Americans to treat the hypercholesterolemia [1]. Currently marketed statins in the US include simvastatin, lovastatin, atorvastatin, fluvastatin, pravastatin, rosuvastatin, and pitavastatin. Although statins are generally well-tolerated, patients concomitantly receiving multiple medications are at an increased risk of adverse events including myalgia, myopathy and rhabdomyolysis, due to increased exposure of statins causing by drug interactions in the presence of co-medications [2]. For example, in a cross-sectional study of 2742 dyslipidemia patients, a total of 198 statin-related drug-drug interactions (DDIs) were identified (7.2%) among those aged 54–75 years who were receiving a mean of 3.8 and 5.8 concomitant medicines [3]. Thus, it is crucial to consider DDI risks when co-administering other drugs in patients receiving statin therapy. Mechanisms that cause statin-related DDIs should be understood for risk management.

Although statins have similar mechanism of action, their disposition pathways differ [4]. Lipophilic statins, including simvastatin, lovastatin, atorvastatin, and fluvastatin, are extensively metabolized by CYP3A4 or CYP2C9. Hydrophilic statins, including pitavastatin, pravastatin and rosuvastatin, are mainly eliminated unchanged with minimal metabolism by CYP enzymes [5]. Drug transporters in the liver, intestine, and kidneys can also influence the disposition of statins. All statin drugs are substrates of the

membrane transporter organic anion transporting polypeptide 1B1 (OATP1B1) (encoded by *SLCO1B1*) [6–9]. Pharmacogenetic studies in statin taking patients with different *SLCO1B1* polymorphisms have revealed that systemic exposure of most statins were significantly increased in patients with genotype *SLCO1B1* c.521 CC, a polymorphism with reduced OATP1B1 function [10]. The rank order of mean systemic exposure change (in fold) of various statins in subjects with variant alleles as compared to wild type are as follows: simvastatin (4.8) > pitavastatin (3.3) > atorvastatin (3.2) > pravastatin (2.0) > rosuvastatin (1.6) > fluvastatin (1.1), indicating the importance of OATP1B1 in the disposition of some statins [11, 12]. Because different transporters and CYP enzymes contribute to the disposition of different statins, the exposure change of each statin by the same perpetrator (inhibitor) drug can be quite different. As such, quantitative prediction of statin DDI is complicated.

Elsby et al. developed a static model to predict the AUC change of statins in the presence of transporter or enzyme inhibitors [13]. By adopting the extended clearance concept [14], we developed mechanistic static models for all 7 U.S.-marketed statins to predict DDIs in the presence of enzyme and/or transporter inhibitors (unpublished) [15]. Our analysis showed that 60% (33/56 DDI cases) of predicted AUC ratios of statin AUC in the presence and absence of inhibitors (AUCRs) were within 80–125% of the observed AUCRs. While static models are relatively straightforward to apply, they are not able to consider the dynamic concentrations of victim (substrate) drugs and inhibitors, especially concentrations in different tissues with varying expression levels of transporters or enzymes. These limitations hinder quantitative understanding and prediction of DDIs involving multiple transporters or complex enzyme-transporter interplay [16].

Physiologically based pharmacokinetic (PBPK) models integrate human physiologically-dependent system parameters with drug-dependent parameters to predict drug pharmacokinetics in the presence of intrinsic or extrinsic factors [17]. The use of PBPK to assess DDIs mediated by drug transporters is emerging, especially in studying the role of OATPs in the disposition of statin drugs [18–20]. For example, the development of PBPK models for rosuvastatin, pravastatin, and simvastatin have been reported previously [19, 21, 22].

To establish a framework to evaluate statin-associated risk, we developed PBPK models for pitavastatin and atorvastatin using *in silico*, *in vitro* and human pharmacokinetic data. These models considered quantitative contribution from both enzymes and transporters to the disposition of these drugs. We then used these models to simulate statin pharmacokinetic in subjects with varying *SLCO1B1* polymorphism or in subjects co-administered

with various CYP enzymes and/or transporter inhibitors. The results (1) quantified key factors that determined the disposition of these two statins and confirmed the significant role of OATP1B1, and (2) demonstrated the utility of PBPK in further understanding of knowledge gaps of predicting transporter-based DDIs.

2 Methods

PBPK models were developed using a population-based PBPK software, SimCYP[®] (SimCYP Ltd, a Certara company, Sheffield, UK, Version 14.1). Unless otherwise stated, simulations with virtual population used 5 trials with 10 healthy subjects for each trial (50 subjects in total) in software's built-in healthy volunteer virtual population. For both statins, software's Advanced Dissolution, Absorption, and Metabolism (ADAM) model and permeability-limited liver distribution model were used to parameterize drug absorption and liver disposition, respectively. Data from *in silico*, *in vitro* absorption, distribution, metabolism and excretion (ADME), and observed pharmacokinetic data in healthy subjects with wild type OATP1B1 (encoded by *SLCO1B1*) were used to develop the models (see Sects. 2.1 and 2.2). To simulate the effect of *SLCO1B1* genetic polymorphism, sub-virtual populations were created according to OATP1B1 abundance relative to wild type transporter, named as extensive transporter (ET, see 2.3). To simulate the effect of inhibitors on statin pharmacokinetic profile, inhibitor models from software's drug library or those published in the literature were directly used (See 2.4).

2.1 Pitavastatin Model Development

Pitavastatin drug-dependent parameters are listed in Table 1 and the section focuses on transporter parameterization. In addition to *in silico* and *in vitro* ADME data, the observed mean pharmacokinetic data of pitavastatin in healthy subjects receiving 2 mg pitavastatin via intravenous infusion or 2 mg oral dose (training dataset) [23] were used to optimize several parameters. Hepatic metabolism of pitavastatin is assumed to be rate-limited by hepatic uptake transporters. Direct application of intrinsic clearance ($CL_{int,T}$) values for OATP1B1 and OATP1B3 determined *in vitro* (58.4 and 5.1 $\mu\text{L}/\text{min}/\text{million cells}$, respectively) [24] under-estimated systemic clearance of the drug. As such, empirical scaling factors for OATP1B1 and OATP1B3 were optimized to be 18 and 18, respectively, according to intravenous and oral pharmacokinetic data mentioned above [23].

The final pitavastatin PBPK model was verified by simulating the single oral dose of 4 mg pitavastatin [23], the

exposure changes of pitavastatin in different genotypes of *SLCO1B1*, or in the presence of OATP1B1 inhibitors as described below. The simulated results were compared to the clinical observations to determine the model performance.

2.2 Atorvastatin Model Development

Atorvastatin drug-dependent parameters are listed in Table 1 and the section focuses on transporter parameterization. Because there was no intravenous plasma concentration-time profile data available for atorvastatin, oral pharmacokinetic profiles in healthy subjects [25, 26] were used during model development to optimize intrinsic clearance of hepatic uptake transporter. Atorvastatin is extensively metabolized by CYP3A4 and actively uptaken into hepatocytes through OATP1B1 [27]. Because the uptake process may be the rate-limiting step for the overall clearance of atorvastatin, intrinsic clearance of CYP3A ($CL_{int,CYP3A}$) may be unidentifiable. We tried two approaches to determine $CL_{int,T}$ and $CL_{int,CYP3A}$. First, we obtained $CL_{int,CYP3A}$ by retrograde analysis with reported value of intravenous atorvastatin clearance of 37.5 L/h [28]. The derived $CL_{int,CYP3A}$ was 8 $\mu\text{L}/\text{min}/\text{pmol}$ of recombinant CYP according to the design of the software. (In SimCYP, the unit of $CL_{int,CYP3A}$ is $\mu\text{L}/\text{min}/\text{pmol}$ if obtained from the retrograde method.) Then, we optimized $CL_{int,T}$ for OATP1B1. The optimization began with reported *in vivo* $CL_{int,T}$ of 910 ml/min/kg [29, 30], or 360 $\mu\text{L}/\text{min}/\text{million cells}$ based on software's extrapolation algorithm. The $CL_{int,T}$ can be further used to calculate the maximum transporter-mediated uptake (J_{max}) of atorvastatin (277.2 pmol/min/million cells) based on a Michaelis-Menten Constant (K_m) of 0.77 μM (assuming the lowest atorvastatin K_m value from the reported range of 0.77–15 μM , the University of Washington Metabolism and Transport Drug Interaction Database, UWDiDB). With the input of these parameters, we simulated the pharmacokinetic of atorvastatin after 20 mg single oral administration (training dataset). The initial simulation of atorvastatin over-estimated the AUC, thus an empirical scaling factor of 4 for OATP1B1, obtained by sensitivity analysis using the same training set pharmacokinetic dataset (e.g. plasma concentration-time profile, AUC and C_{max}) after 20 mg oral dosing, was decided [25, 26] (Supplementary Fig. 1). In the second approach, we directly used $CL_{int,CYP3A}$ based on the *in vitro* assays with human liver microsomes (184 $\mu\text{L}/\text{min}/\text{mg}$ protein for ortho-hydro metabolite pathway, and 219 $\mu\text{L}/\text{min}/\text{mg}$ protein for para-hydroxy metabolite pathway, respectively), and then optimized $CL_{int,T}$ as described in the first approach. (In SimCYP, the unit of $CL_{int,CYP3A}$ is $\mu\text{L}/\text{min}/\text{mg}$ protein if the values are obtained from *in vitro* microsome assay. [31]) This modeling approach resulted in similar simulation of atorvastatin pharmacokinetic after 20 mg oral dosing as

Table 1 Drug-dependent parameters for pitavastatin and atorvastatin PBPK models

Pitavastatin			Atorvastatin		
Parameters (Units)	Value	Source and comments	Parameters (Units)	Value	Source and comments
Molecular weight (g/mol)	421.46	[59]	Molecular weight (g/mol)	558.64	[60]
log $P_{o:w}$	2.91	[61]	log $P_{o:w}$	4.07	[62]
Compound type	Monoprotic acid		Compound type	Monoprotic acid	
pKa	5.31	Drugs@FDA[23]	pKa	4.46	[22]
Fraction unbound	0.005	Drugs@FDA[23]	Fraction unbound	0.024	Drugs@FDA [63]
Blood/plasma ratio	0.55	Drugs@FDA[23]	Blood/plasma ratio	0.61	[64]
Absorption model	Advanced Dissolution, Absorption, and Metabolism (ADAM) model	[65]	Absorption model	Advanced Dissolution, Absorption, and Metabolism (ADAM) model	[65]
$P_{eff,man}$ (10^{-4} cm/s)	4.688	GastroPlus ADME Predictor (Simulation Plus, Lancaster, CA). Assuming the solution formulation	Intestinal Breast Cancer Resistance Protein (BCRP) $CL_{int,T}$ (μ L/min)	BCRP: 6	Optimized according to C_{max} and T_{max} in [33]
			$P_{eff,man}$ (10^{-4} cm/s)	Predicted	Apparent permeability of 7.9×10^{-6} cm/s in Caco-2 cells [66]
Distribution model	Full PBPK	[67, 68]	Distribution model	Full PBPK	[67, 68]
$V_{d,ss}$ (L/kg)	0.22	Final value was optimized according to observed value [23] by adjusting $\text{Log}P_{vo:w}$ value with method 2 published by Rodgers et al [68–70] as the prediction model in SimCYP	$V_{d,ss}$ (L/kg)	0.226	Final value was optimized according to observed value [63] by adjusting $\text{Log}P_{vo:w}$ value with method 2 published by Rodgers et al [68–70] as the prediction model in SimCYP
Elimination model	Enzyme kinetics		Elimination model	Enzyme kinetics	
CYPs CL_{int} (recombinant) (μ L/min/pmol)	CL_{int} CYP2C8: 12.98 CL_{int} CYP2C9: 7.93 CL_{int} UGT: 2.52	Retrograde analysis [71] according to 2 mg intravenous pharmacokinetic data[23]. CL_{int} for UGT was directly applied from the in vitro studies [72] because relative contribution of UGT and CYP metabolism is not known. CYPs (CYP2C8 and CYP2C9) contribute to approximately 38% of total enzymatic metabolism. Contribution of CYP2C8 and CYP2C9 were defined based on in vitro phenotyping data [73] (i.e., 35% and 65% for CYP2C8 and CYP2C9, respectively)	CYPs CL_{int} (recombinant) (μ L/min/pmol of isoform)	CL_{int} CYP3A4: 8	Retrograde analysis [71] according to 20 mg PO pharmacokinetic data[25] [26], assuming 100% contribution from CYP3A4
Additional clearance (μ L/min/mg protein)	HLM CL_{int} : 1452.69	Estimated by the retrograde analysis in SimCYP			

Table 1 continued

Pitavastatin			Atorvastatin		
Parameters (Units)	Value	Source and comments	Parameters (Units)	Value	Source and comments
Renal clearance CL_R (L/h)	0.129	[23]	Renal clearance CL_R (L/h)	0.375	[28]
Liver transporters $CL_{int,T}$ (μ L/min/million cells)	OATP1B1 $CL_{int,T}$: 58.4 ^a Empirical scaling factor: 18 ^b OATP1B3 $CL_{int,T}$: 5.1 ^a Empirical scaling factor: 18 ^b CL_{PD} : 11 ^a	Refer to footnote	Liver transporters $CL_{int,T}$ (μ L/min/million cells)	OATP1B1 J_{max} : 277.2 K_m : 0.77 μ M ^c Empirical scaling factor: 4 ^d $CL_{int,T}$ BCRP: 1.4 ^e CL_{pd} : 17 ^f	Refer to footnote

BCRP breast cancer resistance protein, CL_{PD} passive diffusion clearance, CL_R renal clearance, CL_{int} intrinsic clearance of enzyme, $CL_{int,T}$ intrinsic clearance of transporter, *CYPs* Cytochromes P450, *HLM* human liver microsomes, $LogP_{o:w}$ logarithm of the *n*-octanol:buffer partition coefficient, *pKa* logarithmic constant of acid dissociation constant, *OATP* organic anion transporting polypeptide, $P_{eff, man}$ effective permeability in man, $V_{d,ss}$ steady state volume of distribution, *PO* per os, oral administration, *UGT* Uridine 5'-diphospho-glucuronosyltransferase (UDP)-glucuronosyltransferase

^a [24]

^b Optimized per method section

^c The University of Washington Drug Interaction Database

^d Optimized per method section

^e [34]

^f [74]

Approach 1, suggesting that $CL_{int,CYP3A}$ is unidentifiable and hepatic uptake seems to be the rate-limiting step of the overall clearance of atorvastatin.

Atorvastatin is a substrate of Breast Cancer Resistance Protein (BCRP) encoded by *ABCG2*, and Keskitalo et al [32] found that subjects with the *ABCG2* c.421AA genotype showed a 72% and 46% increase in atorvastatin AUC and C_{max} , respectively, as compared to subjects with the c.421CC genotype, suggesting the important role of BCRP in the absorption/disposition of atorvastatin. However, due to the limited data, BCRP and OATP transport CL_T could not be simultaneously fitted with certainty, particularly using oral data alone. Because the $t_{1/2}$ of the atorvastatin was not changed in the *ABCG2* genotype, we assume that BCRP mainly plays a role in the absorption of atorvastatin. The intrinsic clearance of atorvastatin via intestinal BCRP was optimized manually to match the simulated C_{max} and time to C_{max} (T_{max}) to those reported in the literature [33]. The contribution of biliary clearance of atorvastatin from BCRP was directly adopted from the in vitro hepatocyte uptake studies (1.4 μ L/min/mg protein, assuming 1 million cell = 1 mg protein) [34], which appears to contribute minimally to overall hepatic clearance.

The final atorvastatin PBPK model was verified by simulating the single oral dose of 40 mg [35], the exposure changes of atorvastatin in different genotypes of *SLCO1B1*, or in the presence of CYP3A and OATP1B1 inhibitors as described below. The simulated results were compared to the clinical observations to determine the model performance.

2.3 Simulation of Exposure Change of Statins in Populations with Different Genotypes of *SLCO1B1*

In SimCYP, the $CL_{int,T}$ of transporter is scaled to whole organ clearance by multiplying a series of scaling factors including milligram microsomal protein per gram of liver (MPPGL), transporter abundance (abundance of various transporter allelic variants), and total liver weight. Different *SLCO1B1* genotypes include ET (extensive transporter), IT (intermediate transporter), PT (poor transporter), and UT (ultra-rapid transporter). For our studies described in this manuscript, all population simulations were conducted by using SimCYP-defined virtual healthy population, unless otherwise specified

(e.g., simulations in populations with *SLCO1B1* c.521 TT or c.521 CC). For a virtual healthy population, the percentage of each transporter phenotype in a population would be determined by the frequency values of transporter phenotype under transporter phenotype table in SimCYP virtual population, which are 0.64, 0.02, 0.27, and 0.07 for ET, PT, IT, and UT, respectively. The default relative abundance values for each *SLCO1B1* genotype are 1, 0.68, 0.37, and 1.47 for ET, IT, PT, and UT, respectively. This relative abundance determines OATP1B1 intrinsic clearance in non-ET subjects as a fraction of that in ET in simulations of the pharmacokinetic of statins in these subjects.

We assumed that population with *SLCO1B1* c.521 TT was consisted of subjects with 100% of ET, and population with *SLCO1B1* genotype c.521 CC was consisted of subjects with 100% of PT. Two populations were created separately for *SLCO1B1* genotype c.521 TT population and *SLCO1B1* genotype c.521 CC population by adjusting the population frequency of ET or PT to 1 while keeping all other values as 0, respectively. The plasma concentration-time profile of pitavastatin or atorvastatin in *SLCO1B1* genotype c.521 TT or in *SLCO1B1* genotype c.521 CC was simulated in each respective population (5 trials with 10 subjects in each trial).

2.4 Inhibitor Drug Models

Models for itraconazole and its metabolite hydroxyl-itraconazole were directly used from SimCYP software compound library. Erythromycin PBPK model parameters were adopted from the model published by Yeo et al. [36]. Gemfibrozil PBPK inhibitor model published by Varma et al. [37] (with the consideration of its metabolite gemfibrozil 1-*O*- β -glucuronide) was directly applied as the inhibitor model. Cyclosporine model from Jamei, et al [21] and rifampin model from Varma et al [38] were directly applied (also see Sect. 2.6). The inhibitory kinetic parameters on CYP enzymes and transporters for these inhibitors are shown in Table 2.

2.5 Measurement of Prediction Performance

Both atorvastatin and pitavastatin have significant inter-study variability in pharmacokinetics [39]. As such, we used AUC ratios (with/without co-medication or between different genotypes) as metrics to evaluate model performance. Effect of *SLCO1B1* polymorphism was measured by statin AUC ratio (AUCR), the ratio between mean statin AUC in PT subjects to that in ET subjects. The magnitude of drug interaction was represented by AUCR (mean AUC of statin in the presence of an inhibitor drug compared to the mean AUC in the

absence of an inhibitor drug). The prediction performance of PBPK models was determined by an R value (R is the ratio of mean simulated AUCR to mean observed AUCR, $R = \text{AUCRs}/\text{AUCRo}$). There is no consensus with regard to acceptance criteria of a PBPK model [40]. A criterion that predicted pharmacokinetic parameters within twofold of the observed data has been used frequently to assess the performance of a PBPK model [40]. Although this twofold criterion is arbitrary, for the purpose of our analysis and known inter-study variability, an R value within a twofold range (0.5–2.0) was regarded satisfactorily. Furthermore, when observed plasma concentration-time profiles were available, the models were considered acceptable if the clinical observations were within 90% confidence interval (CI) of the simulated mean plasma concentration curve, an approach used in other PBPK studies [41, 42]. The similar analysis on change in C_{max} as a result of DDI or different genotypes of *SLCO1B1* was conducted and the results were shown in Supplementary Table 1.

2.6 Evaluation of the Impact of Inhibitor K_i for OATP1B1 on DDI Prediction

For DDI prediction with rifampin and cyclosporine, a sensitivity analysis on their K_i for OATP1B1 was conducted by changing the K_i value to up to 100 fold-lower used in the published models. SimCYP's built-in sensitivity analysis function was used to conduct the sensitivity analysis.

3 Results

3.1 Performance of Pitavastatin and Atorvastatin Models for Predicting Pharmacokinetic Profiles via Intravenous and Oral Routes of Administration

Figure 1 shows that the pitavastatin substrate model described pitavastatin pharmacokinetic profile after single intravenous infusion of 2 mg (Fig. 1a), which was used during model development to optimize several parameters (Table 1) [23]. The model was also able to independently describe pitavastatin pharmacokinetic profiles after single oral doses of 2 mg and 4 mg in healthy subjects (Fig. 1b, c) [23].

Figure 2 shows that the atorvastatin substrate model well described atorvastatin pharmacokinetic profile following 20 mg [25] or 40 mg of single oral administration in healthy subjects [35], in which 40 mg data set was not used during the model development.

Table 2 Inhibitor PBPK models

Inhibitor PBPK models	Inhibitory kinetic parameters		Source
Itraconazole	Inhibition on CYP3A4: K_i of competitive inhibition: 0.0013 μM	Inhibition on transporter: N/A	Built-in SimCYP inhibitor model
Erythromycin	Inhibition on CYP3A4: K_i of competitive inhibition: 82 μM K_i of mechanism-based inhibition: 2.25 μM	Inhibition on OATP1B1: K_i of competitive inhibition: 1.67 μM	[75]
Gemfibrozil	Inhibition on CYP2C8: K_i of competitive inhibition: 9.3 μM	Inhibition on OATP1B1: K_i of competitive inhibition: 2.5 μM	[19, 37]
Gemfibrozil metabolite: gemfibrozil 1- <i>O</i> - β -glucuronide	Inhibition on CYP2C8: K_i of competitive inhibition: 10.1 μM	Inhibition on OATP1B1: K_i of competitive inhibition: 7.9 μM	[19, 37]
Rifampin	K_i of competitive inhibition on CYP2C8: 30.2 μM K_i of competitive inhibition on CYP3A4: 18.5 μM CYP3A4 induction: CYP3A4 E_{max} 49.5; CYP3A4 EC_{50} 0.229 μM	Inhibition on transporters: K_i of competitive inhibition on OATP1B1: 0.93 μM K_i of competitive inhibition on OATP1B3 ¹ : 0.3 μM	[38]
Cyclosporine	K_i of competitive inhibition on CYP3A4: 12.7 μM	Inhibition on transporters: K_i of competitive inhibition on OATP1B1: 0.014 μM K_i of competitive inhibition on OATP1B3: 0.007 μM K_i of competitive inhibition on BCRP: 0.28 μM	[21, 76]

¹ In vitro K_i for OATP1B3 by rifampin ranges from 0.22–5 μM , here the value of 0.3 μM was used based on one of the in vitro inhibition studies with pitavastatin as the probe [77]

3.2 Simulation of Exposure Change in Populations with Different Genotypes of *SLCO1B1*

Simulation of the effect of *SLCO1B1* polymorphism on systematic exposure of pitavastatin or atorvastatin was conducted under the assumptions of relative transporter abundance with *SLCO1B1* genotypes as described in Methods. Both pitavastatin and atorvastatin models predicted an exposure change in the presence of *SLCO1B1* polymorphism to be within twofold of the observed values

(Table 3). The pitavastatin model slightly under-estimated the change in C_{max} as a result of different *SLCO1B1* genotypes (R value is 0.39) (Supplementary Table 1).

3.3 DDI Prediction

The predicted mean AUCRs and $C_{\text{max}}R$ for DDIs with gemfibrozil, itraconazole, and erythromycin were within two-fold of observed values (Table 3) (Supplementary Table 1). Figure 3 and Table 3 compared the simulated

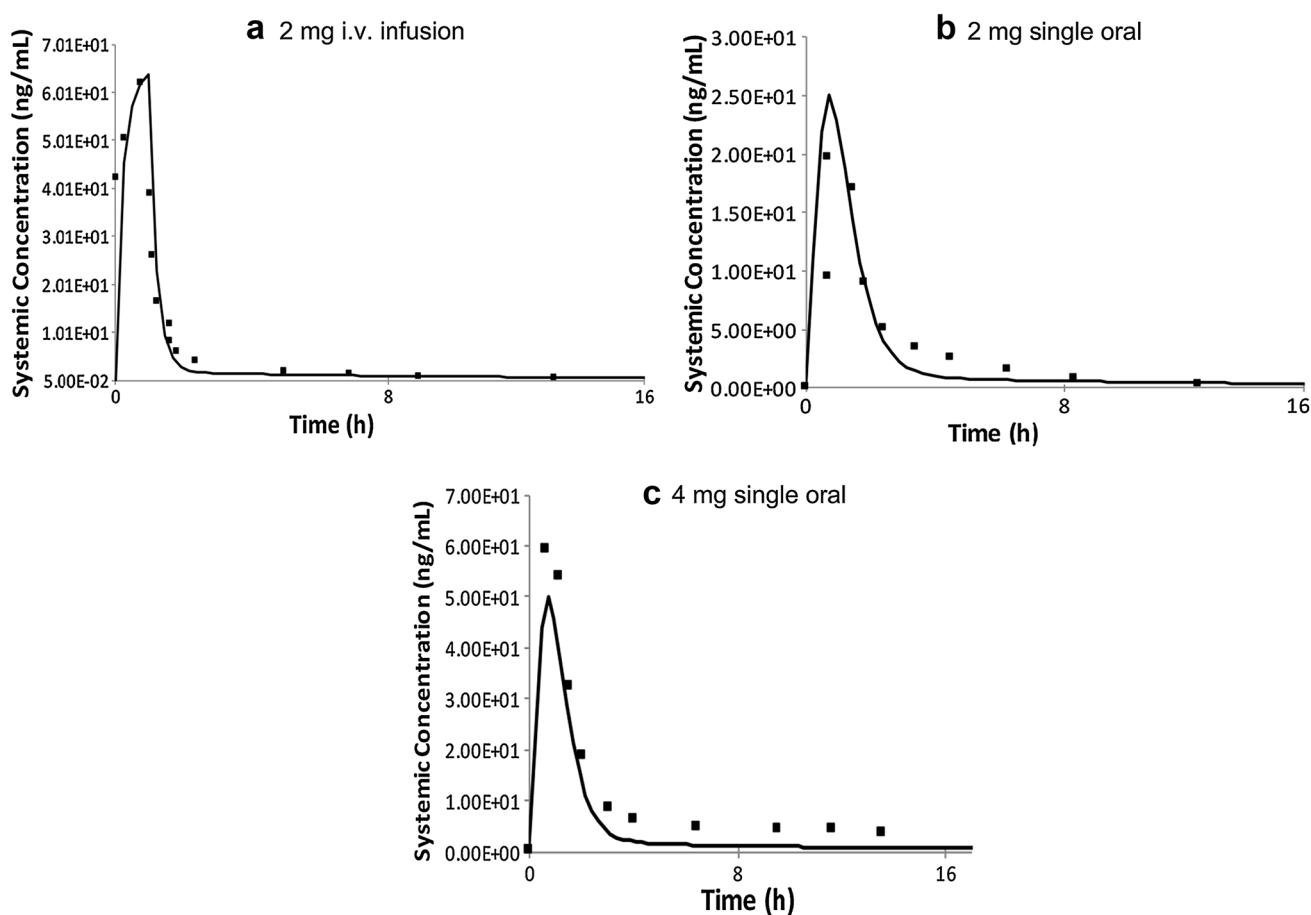


Fig. 1 The simulation of plasma concentration-time profile of pitavastatin. Simulation of pitavastatin pharmacokinetic profile using the PBPK model (mean profile) following **a** intravenous infusion of 2 mg pitavastatin (model development), **b** single oral administration

of 2 mg and **c** single oral dose of 4 mg pitavastatin (model verification). Simulations were conducted with virtual healthy subjects as described in Methods. Data points are observed mean values [23]

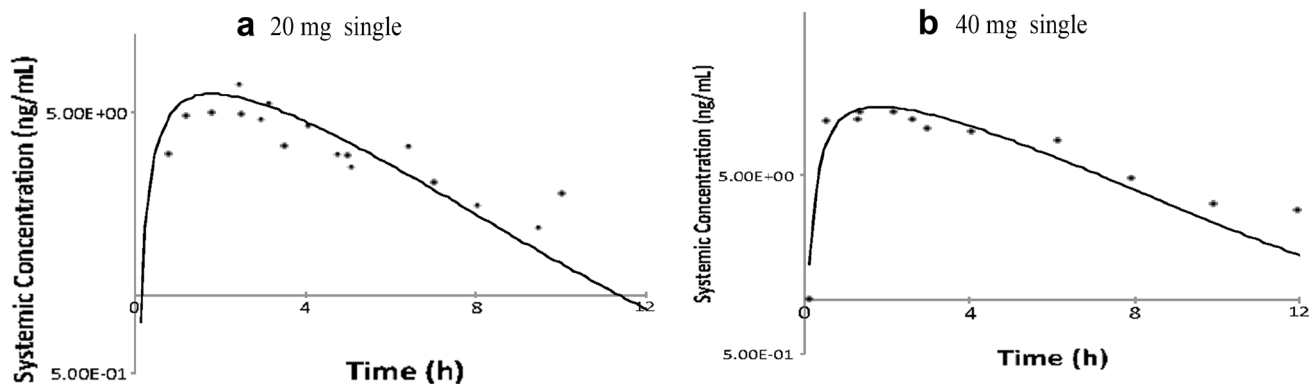


Fig. 2 The simulation of plasma concentration-time profile of atorvastatin. Simulation of atorvastatin pharmacokinetic profile using the PBPK model (mean profile) following a single oral dose of 20 mg atorvastatin (model development) (**a**), and a single oral dose of 40 mg atorvastatin (model verification) (**b**). Data points are observed mean

values (20 mg [25, 26], 40 mg [35]). Simulations were conducted with virtual healthy subjects as described in Methods. Data from two different studies (with 20 mg) [25, 26] were presented by *different symbols*

and observed pharmacokinetic profiles of pitavastatin and atorvastatin, respectively, in the presence of gemfibrozil.

The simulated pitavastatin or atorvastatin plasma concentration-time profiles in the presence of cyclosporin (200 mg co-administrated with pitavastatin [23], 5.2 mg/kg

Table 3 The effect of *SLCO1B1* polymorphism or inhibitors on AUC changes of atorvastatin or pitavastatin

Variable	<i>SLCO1B1</i> polymorphism or inhibitor drug			Pitavastatin			
	Atorvastatin	Observed AUC ^a	R value AUCs/AUCRo	Predicted AUCR	Observed AUCR	R value AUCs/AUCRo	
0.5 < AUCRs/AUCRo < 2.0	<i>SLCO1B1</i> polymorphism (c.521 CC vs c.521 TT)	1.90 (1.48–2.39)	2.44 (1.36–4.69) [48]	0.78	1.80 (1.46–2.18)	3.08 (2.14–4.16) [47]	0.58
	Gemfibrozil	1.55 (1.43–1.63)	1.24 (0.99–1.50) [26]	1.25	2.27 (2.18–2.37)	1.25 (1.06–1.50) [23]	1.82
	Itraconazole	1.73 (1.56–1.83)	2.40 (1.50–2.50) [78]	0.72	N/A	N/A	N/A
	Erythromycin	2.44 (2.12–2.53)	1.33 (1.06–1.65) [25]	1.83	N/A	N/A	N/A
	Rifampin	2.11 (1.95–2.21)	6.80 (4.40–9.20) [79]	0.31	2.15 (2.05–2.25)	6.74 (4.73–8.74) [80]	0.32
AUCRs/AUCRo < 0.5 (with unmodified K_i)	Rifampin with modified K_i	7.77 (6.54–8.03)	6.80 (4.40–9.20) [79]	1.14	6.37 (5.85–6.92)	6.74 (4.73–8.74) [80]	0.94
	Cyclosporine	1.87 (1.65–1.99)	7.45 (7.41–7.47) [43]	0.25	1.91 (1.86–1.97)	4.60 (4.00–5.10) [23]	0.41
	Cyclosporine with modified K_i	6.40 (4.93–6.82)	7.45 (7.41–7.47) [43]	0.86	4.73 (4.36–5.13)	4.60 (4.00–5.10) [23]	1.02

AUC area under the concentration-time curve, AUCR ratio of AUC, *R value* AUCs/AUCRo (ratio of mean predicted AUCR and mean observed AUCR); K_i inhibitor constant, *SLCO1B1* or *OATP1B1* organic anion transporting polypeptide 1B1

^a AUCR refers to the ratio between the AUC of statins comparing variant OATP1B1 to wild type or in the presence and absence of an inhibitor drug. The range in the parenthesis is 95% confidence interval of AUCR

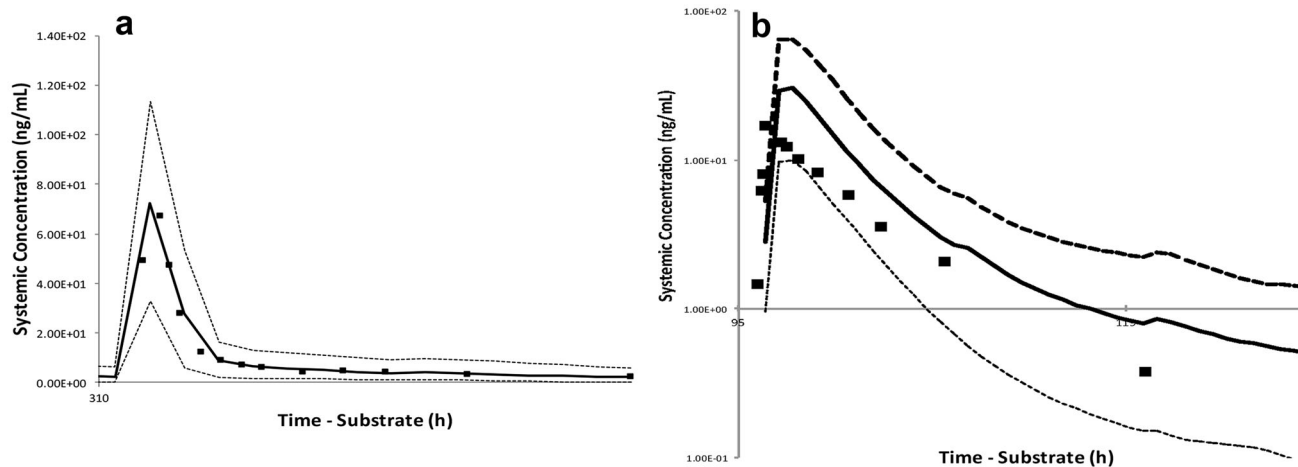


Fig. 3 a Simulation of pitavastatin pharmacokinetic profile when the drug is coadministered with gemfibrozil. Mean plasma concentration-time profile of oral administration of 4 mg pitavastatin in the presence of 600 mg gemfibrozil. *Squares* represent mean observed plasma concentration-time profile of pitavastatin dosed in the presence of gemfibrozil. *Dotted line* represents 5th and 95th percentile of simulated mean data, respectively. Observed data were from Drugs@FDA [23]. **b** Simulation of atorvastatin pharmacokinetic

profile when the drug is coadministered with gemfibrozil. Mean plasma concentration-time profile of oral administration of 40 mg atorvastatin in the presence of 600 mg gemfibrozil. *Squares* represent mean observed plasma concentration-time profile of atorvastatin dosed in the presence of gemfibrozil. *Dotted line* represents 5th and 95th percentile of simulated mean data, respectively. Observed data were from Ref. [81]

co-administrated with atorvastatin[43] or in the presence of single intravenous infusion or oral dose of rifampin (600 mg) significantly under-estimated the observed magnitude of clinical DDI (Table 3). The *R* values of AUCR (See Sect. 2.6) for pitavastatin co-administered with rifampin and cyclosporine were 0.32 and 0.41, respectively; and *R* values of AUC for atorvastatin co-administered with rifampin and cyclosporine were 0.31 and 0.25, respectively (Table 3). Similar under-estimation in the change of C_{max} was found for atorvastatin DDI with

rifampin and cyclosporine, or pitavastatin DDI with cyclosporine (Supplementary Table 1).

3.4 Evaluation of Inhibitor K_i for OATP1B1 on the Performance of DDI Prediction

The significant under-predictions with rifampin and cyclosporine may be caused by several factors. To explore one potential factor, we conducted sensitivity analyses by assuming that OATP1B1 inhibition potency in both

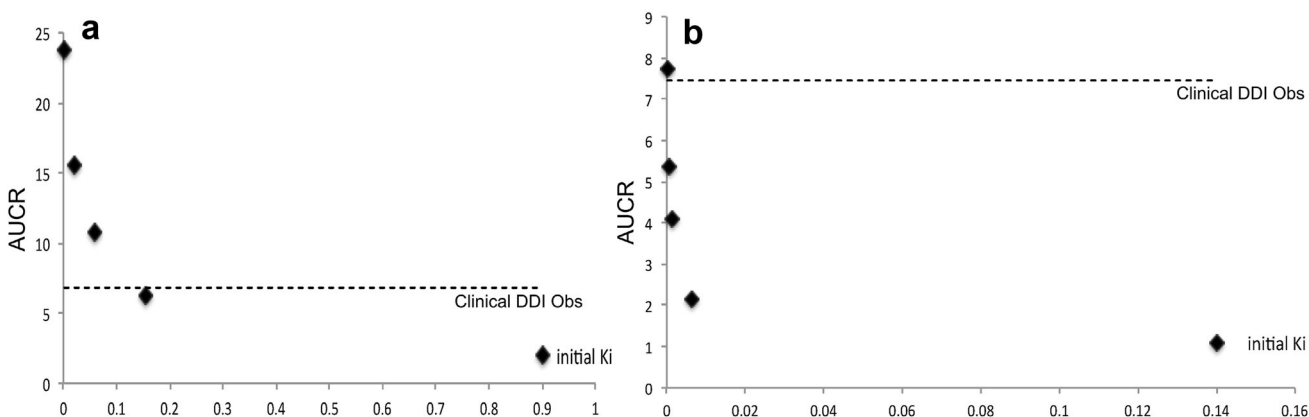


Fig. 4 The impact of different K_i values for OATP1B1 on AUCR of atorvastatin DDI with rifampin (a) and cyclosporine (b). Automatic sensitivity analysis (ASA) of the K_i values of rifampin (a) and cyclosporine (b) for OATP1B1 inhibition was conducted with SimCYP stimulator V14.1 using pitavastatin or atorvastatin PBPK models with rifampin or cyclosporine as the inhibitor drugs, respectively. The predicted AUCR was plotted with the

corresponding K_i used in ASA. The K_i used from the published model was marked with “initial K_i ” in the figure. K_i inhibitory constant, *OATP* organic anion transporting polypeptide, *AUCR* ratio of area under the concentration-time curve, *PBPK* physiologically based pharmacokinetic, *ASA* automatic sensitivity analysis, *DDI* drug-drug interaction, *Obs* observed

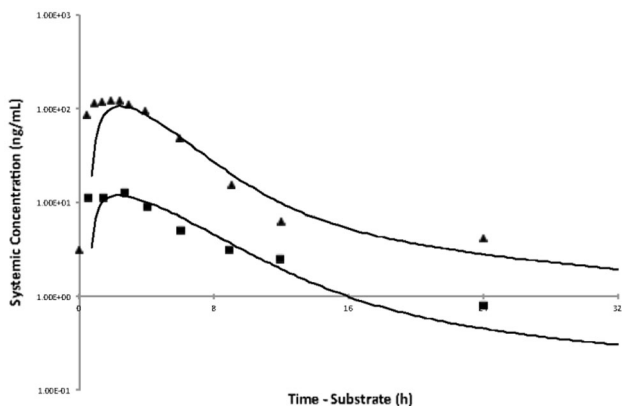


Fig. 5 Simulation of atorvastatin-rifampin drug-drug interaction with OATP1B1 K_i of 0.09 μM . Mean (solid line) plasma concentration-time profile of oral administration of 40 mg atorvastatin in the presence of single intravenous infusion of 600 mg rifampin. Triangles and squares represent mean observed plasma concentration-time profile of atorvastatin dosed in the presence or absence of rifampin, respectively. The K_i of rifampin on OATP1B1 was lowered by tenfold to 0.09 μM from the initial 0.9 μM . Observed data were from Ref. [79]. OATP organic anion transporting polypeptide, K_i inhibitory constant

inhibitors' PBPK models may be lower than the actual inhibition potency in vivo. The K_i values for OATP1B1 used in models were adopted from publically reported values of 0.014 and 0.9 μM for cyclosporine [44] and rifampin [19], respectively. However, a wide range of K_i values for OATP1B1 have been reported for cyclosporine

and rifampin (0.014–1.0 and 0.41–3.1 μM , respectively based on UWDiDB). The analyses showed that decreasing initial K_i values by tenfold for both rifampin and cyclosporine significantly improved the DDI prediction (Table 3; Fig. 4). For AUCR, the R values of atorvastatin DDI using these modified K_i values were 0.86 and 1.14 for cyclosporine and rifampin, respectively; the R values of pitavastatin DDI using these modified K_i values became 1.02 and 0.94 for cyclosporine and rifampin, respectively (Table 3). For $C_{\text{max}}R$, the modification in K_i improved the predictions, with the R values of atorvastatin DDI became 0.68 and 1.33, for rifampin and cyclosporine, respectively; while the R values of pitavastatin DDI using these modified K_i values became 0.48 for cyclosporine. Figures 5 and 6 show the simulated concentration-time profiles of atorvastatin and pitavastatin in the presence of rifampin with the modified K_i value, respectively, which were close to the clinical observations.

4 Discussion

4.1 Performance of Statin PBPK Models

In this study, we developed substrate PBPK models for pitavastatin and atorvastatin, with the consideration of the contributions from both enzymes (CYP2C9/2C8/UGT for pitavastatin and CYP3A4 for atorvastatin) and transporters

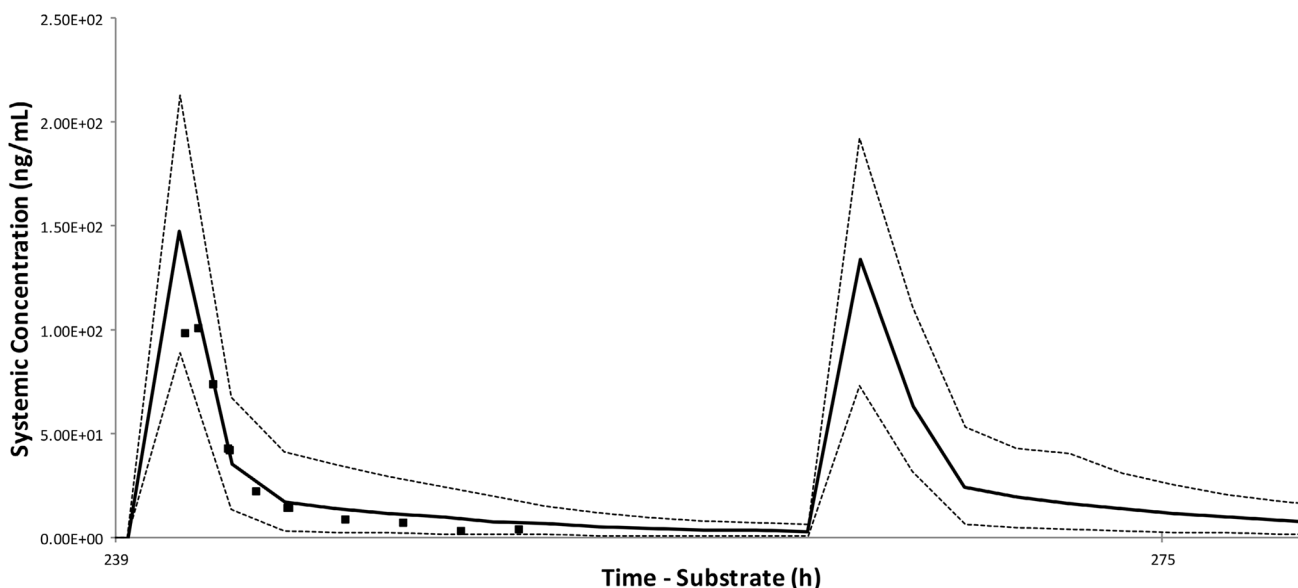


Fig. 6 Simulation of pitavastatin DDI with rifampin using a K_i value of 0.09 μM for OATP1B1 inhibition. Mean (solid line) plasma concentration-time profile of oral administration of 4 mg pitavastatin in the presence of single oral dose of 600 mg rifampin. Squares represent mean observed plasma concentration-time profile of pitavastatin dosed in the presence of rifampin. The K_i of rifampin

on OATP1B1 was lowered by tenfold to 0.09 μM from the initial K_i of 0.9 μM . The dashed lines are 95th and 5th percentile of simulated mean data, respectively. Observed data was taken from Ref. [23]. OATP organic anion transporting polypeptide, K_i inhibitory constant, AUC area under the concentration-time curve

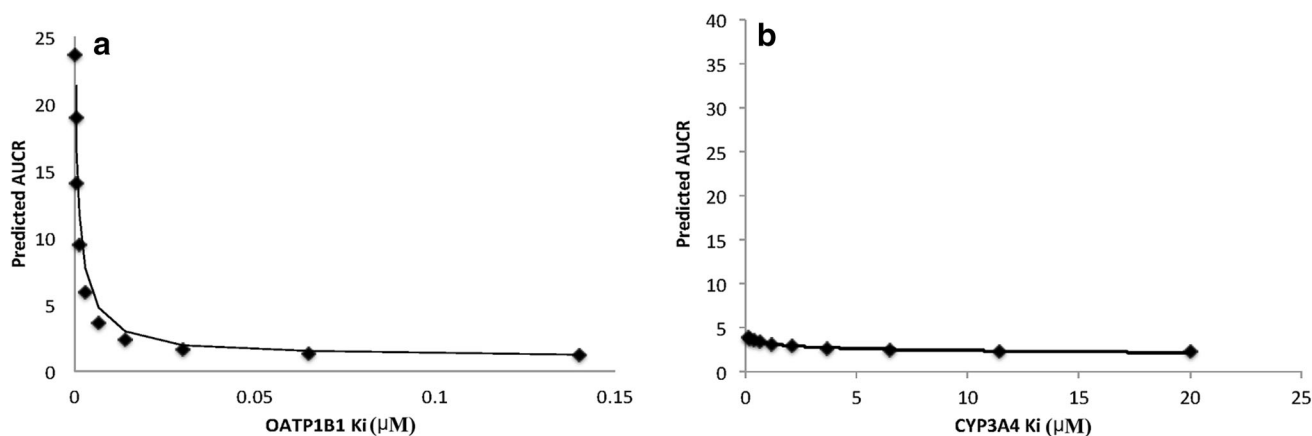


Fig. 7 The impact of inhibition of OATP1B1 (a) and CYP3A4 (b) on the predicted AUCR of atorvastatin DDI with cyclosporine. With atorvastatin PBPK model as the substrate model and cyclosporine as the inhibitor model, sensitivity analysis on OATP1B1 K_i (a) or CYP3A4 K_i (b) was conducted, respectively. The different OATP1B1

K_i or CYP3A4 K_i values were plotted with corresponding predicted AUCR. K_i inhibitory constant, OATP organic anion transporting polypeptide, AUCR ratio of area under the concentration-time curve, PBPK physiologically based pharmacokinetic, CYP cytochrome P450

(OATP1B1/3 for pitavastatin and OATP1B1/BCRP for atorvastatin). Due to limitations in in vitro-in vivo extrapolation (IVIVE) of transporter-mediated clearance, scaling factors (e.g. intersystem extrapolation factor (ISEF) or empirical scaling factor) are frequently applied during PBPK model development to capture the observed in vivo clearance [45]. As shown by Jones et al, a wide range of scaling factors were needed for each of 7 substrate drugs investigated (including some statins), suggesting significant gaps in translating in vitro transporter kinetic data using PBPK models. This gap cannot be filled with a common scaling factor [46]. For the pitavastatin model, we used the $CL_{int,T}$ for OATP1B1 and OATP1B3 measured in hepatocytes, which were 58.4 and 5.1 $\mu\text{L}/\text{min}/\text{million cells}$, respectively [24]. The difference in $CL_{int,T}$ suggests that the fractions of transporter for OATP1B1 and OATP1B3 are different, and OATP1B1 is the major transporter for hepatic uptake of pitavastatin. The initial model with these in vitro parameters cannot describe the clinically observed 2 mg oral dose or intravenous pharmacokinetic data, and the same empirical factor of 18 for OATP1B1 and OATP1B3 has to be applied to capture clinical data. For atorvastatin, we found that we need to apply a scaling factor of 4 to $CL_{int,T}$ of OATP1B1 (presented in J_{max} and K_m) obtained from hepatocyte study in order to recapitulate clinical observation.

Clinical studies showed that the exposure of pitavastatin increased by 3.1-fold in subjects with *SLCO1B1* c.521 CC (PT) genotype as compared to those with the wild type c.521 TT (ET) [47]. Similarly, an increase of 2.4-fold in the exposure of atorvastatin was found in subjects with the *SLCO1B1* c.521 CC genotype as compared to those with the wild type [48]. The reduced function of OATP1B1 in subjects with genotype

SLCO1B1 c.521 CC could be considered as a genetic specific inhibition of OATP1B1, which would be considered as a more specific impairment of OATP1B1 function. Predictions of the AUCR based on different *SLCO1B1* genotypes indicated that the current PBPK models appear to describe the contribution of OATP1B1 to the disposition of these two statins. The predicted AUCR in DDI studies with gemfibrozil, itraconazole, and erythromycin were within twofold range of clinically observed AUCR. The good predictions of DDIs with multiple inhibitors that inhibit enzymes and/or transporter OATP1B1 further lend confidence of the final substrate PBPK models.

Besides being a substrate of OATP1B1, atorvastatin is also metabolized by CYP3A, and thereby, it is interesting to know which pathway (OATP1B1 or CYP3A) is the rate-limiting step of atorvastatin elimination. A sensitivity analysis was conducted on the K_i of OATP1B1 and CYP3A4, respectively (Fig. 7). If decreasing the K_i of cyclosporine for OATP1B1 by 100-fold, the change in predicted AUCR could be as large as tenfold (a steeper slope), while same fold-change (100-fold) in its K_i for CYP3A4 only resulted in a 1.6-fold change in the predicted AUCR (a flatter slope). Thus, the data suggested that in the presence of a drug inhibiting both CYP3A4 and OATP1B1, systemic exposure of atorvastatin was more affected by OATP1B1 inhibition than by CYP3A4 inhibition. This sensitivity analysis supported that OATP1B1 was the rate-limiting step for the hepatic clearance of atorvastatin. Our observation is consistent with the findings from Maeda et al [49]. In their study, the exposure of atorvastatin increased 12-fold in the presence of the OATP1B1 inhibitor rifampin, but did not change in the presence of the strong CYP3A4 inhibitor itraconazole.

Despite the encouraging results of independent verification of PBPK models of pitavastatin and atorvastatin with regard to *SLCO1B1* polymorphism and DDI with some inhibitors (itraconazole, erythromycin, and gemfibrozil), significant under-predictions were observed when published cyclosporine and rifampin PBPK models were directly used to simulate their effects on the exposure of pitavastatin and atorvastatin (Table 3). The simulated inhibitor pharmacokinetic profile of rifampin or cyclosporine is close to clinical observation, which excludes the possibility that the poor prediction of DDI is as a result that inhibitor model had not been adequately developed (Supplementary Fig. 2). Similar under-prediction of DDI with cyclosporine was also found in other published PBPK models. The published pravastatin PBPK model under-estimated the clinical cyclosporine-pravastatin DDIs, when the reported geometric mean in vitro K_i was used in cyclosporine model [19]. The rosuvastatin PBPK model developed by Jamei et al [21] also seemed to under-estimate the clinically observed rosuvastatin-cyclosporine DDIs. In a recent PBPK analysis, Snoeys and colleagues also updated rifampin PBPK model with K_i for OATPs that are approximately tenfold lower than those reported by others in order to predict the risk of clinical DDI [50]. Recently, Zhang et al. developed an atorvastatin PBPK model to predict PK of atorvastatin and its two metabolites and the effect of CYP3A modulators on atorvastatin pharmacokinetic. The author demonstrated reasonable prediction of the effect of single dose rifampin on atorvastatin pharmacokinetic, primarily via OATP inhibition; however, the author stated that OATP parameters were “optimized with the data from combination with a single dose of rifampin” and no details on the optimization and K_i of inhibitor were given. Furthermore, although the predicted AUCR as a result of rifampin DDI was similar to observation in Zhang et al.’s model, the change in C_{max} is significantly under-estimated (5.7 predicted vs. 12.7 observed). In our study, we demonstrated that OATP K_i values for cyclosporine and rifampin need to be lowered by tenfold in order to predict their effects on the pharmacokinetics of pitavastatin and atorvastatin (Table 3). With a lower K_i , the predicted AUCR and change in C_{max} are close to clinical observation.

In addition to OATP inhibition potency, other reasons may contribute to under prediction of cyclosporine-statin or rifampin-statin DDI. First, the current DDI simulations were conducted in healthy subjects, while the exposure of cyclosporine may differ between heart transplant patients and virtual healthy subjects [51]. Second, for both statin substrates, we directly used hepatic passive diffusion clearance (CL_{pd} , Table 1) based on in vitro findings, whereas we optimized empirical scaling factor values for active uptake processes only. Both passive and active

uptake clearances are important in determining drug exposure in the liver, and one cannot completely rule out the possibility of a lower or a higher in vivo CL_{pd} . Models with lower CL_{pd} may require higher $CL_{int,T}$ by OATP to describe observed pharmacokinetic profiles during model development. Consequently, simulated genetic effect and DDI may be greater. If so, one can imagine the amount of additional simulations needed to investigate relative contribution of hepatic uptake by CL_{pd} and transporter $CL_{int,T}$. Third, concurring disposition pathways that may be affected by cyclosporine and rifampin have not been appropriately incorporated in the model for pitavastatin and atorvastatin. For example, we did additional sensitivity analysis to investigate the effect of lowering OATP1B1 K_i of cyclosporine on predicted DDI with pravastatin and rosuvastatin. As described above, the pravastatin model under-estimated the clinically observed pravastatin-cyclosporine DDI [19]. Although lowering the OATP1B1 K_i of cyclosporine slightly increased the predicted AUCR, it failed to fully recapitulate the tenfold clinically observed AUCR (Supplementary Fig. 3). Inhibition of other pathways might contribute to clinically observed AUCR. Cyclosporine is also an inhibitor of MRP2, and MRP2 contributes to the renal clearance of pravastatin, which is not considered in the pravastatin model. Similarly, the tenfold decrease in OATP1B1 K_i from 0.014 μM to 0.0014 μM only slightly increase the simulated AUCR of rosuvastatin from 1.3 fold to around 2.3 fold, and can’t fully recapitulate the clinically observed 7.1 fold change in AUC [21] (Supplementary Fig. 4).

Atorvastatin and pitavastatin have inter-conversion of acid form and lactone forms. However, the administered statin is in acid form, and in clinical studies, acids are major moiety for hepatic uptake by OATPs [27]. Because the main purpose of our modeling is to build a framework to evaluate DDI risk of pitavastatin and atorvastatin with enzyme or transporter inhibitors, we assumed that observed statin plasma pharmacokinetics are representative for the acid form. However, the possible impact of acid-lactone form inter-conversion on clinical DDIs could not be excluded.

In summary, additional analyses are needed to confirm potency of OATP inhibition by cyclosporine and rifampin. In the meantime, one needs to fully characterize disposition mechanisms for substrate drugs and adequately incorporate these mechanisms into PBPK models.

4.2 Using in Vivo DDI Information to Inform DDI Mechanisms

Given the complexity of drug transport process into cells, obtaining accurate inhibitory kinetic parameters with in vitro assays is always challenging, and K_i determined

in vitro is often different from assay to assay, or from laboratory to laboratory. In addition, several studies have shown substrate-dependent inhibition potency for some transporters [52, 53]. A recent study showed substrate-dependent inhibition potency for OATP1B1 while using different probe substrates, for example, estradiol-17 β -glucuronide, estrone-3 sulfate, and sulfobromophthalein [54]. Estradiol-17 β -glucuronide was the most sensitive in vitro OATP1B1 probe substrate among the three substrates tested [54]. It was also shown that for some inhibitors (e.g. cyclosporine, saquinavir, ritonavir), a more complicated inhibitory mechanism (i.e., time-dependent inhibition) on OATP1B1 existed [44, 55]. Pre-incubation of cyclosporine could further potentiate its inhibitory effect on OATP1B1 while testing with several OATP1B1 substrates [44]. Therefore, it may not be appropriate to use a universal “ K_i ” for various victim (substrate) drugs.

PBPK modeling offers a great tool to evaluate the underlying inhibition potency using the observed DDI data, if uncertainties exist. For example, Kato, et al applied PBPK models to estimate in vivo K_i of 11 CYP inhibitors, and found discrepancy between in vitro and in vivo K_i values [56]. Recently, in the cimetidine and metformin PBPK models developed by Burt, et al [57], the clinically observed AUC ratio of DDI could only be recapitulated with the PBPK model while further decreasing cimetidine K_i for OCT2 up to 1000-fold or K_i for both OCT1 and OCT2 up to 500-fold. While an in vitro K_i may not represent in vivo inhibition potency, an apparent “in vivo” K_i could be estimated by fitting the pharmacokinetic prediction to the clinical exposure change of the victim drugs. This approach was applied in the study of Hsu, et al to derive an in vivo inhibition constant on renal transporters by probenecid [58]. The optimized probenecid K_i values on the same renal transporters were different for different victim drugs. We used the similar approach as Hsu, et al to evaluate the influence of K_i on DDI prediction with rifampin and cyclosporine as inhibitors, where “erroneously high” K_i values might be one of the factors for under-prediction. Lowering K_i of rifampin, by tenfold to 0.09 μ M, significantly improved the rifampin-atorvastatin DDI prediction. In vitro data suggested that the K_i value of rifampin for OATP1B1 is similar using either pitavastatin or atorvastatin as the substrate (1.07 μ M vs. 3.08 μ M, respectively) (UWDiDB). Therefore, we used the same modified OATP1B1 K_i and applied it to predict pitavastatin-rifampin DDI. Applying the lower K_i of 0.09 μ M to the rifampin PBPK model improved the prediction for pitavastatin-rifampin DDI as well.

The K_i values for cyclosporine varied 6.3-fold when different OATP1B1 substrates were used in the in vitro transporter inhibition assays [54], suggesting a possible substrate-dependent inhibition of cyclosporine on OATP1B1. The reported K_i of cyclosporine on OATP1B1

used initially in our models was a value optimized with tacrolimus [44]. However, a further decrease in K_i was needed to recapitulate the observed clinical DDI data with our models, suggesting possible substrate-dependent inhibition of cyclosporine on OATP1B1. It is of note that the in vitro K_i of cyclosporine on inhibiting OATP1B1 while using pitavastatin or atorvastatin as the substrates were similar (0.23 μ M with pitavastatin vs. 0.16 μ M with atorvastatin) [54]. Therefore, in our study, we applied the same optimized cyclosporine K_i based on atorvastatin DDI studies to the pitavastatin model that improved prediction.

5 Conclusions

Our PBPK models described the pharmacokinetics of pitavastatin and atorvastatin, and reasonably described systemic exposure change due to OATP1B1 (*SCLO1B1*) polymorphism or clinical DDIs with several OATP1B1 and CYP inhibitors (Table 3). However, DDIs with rifampin and cyclosporine were under-predicted using OATP1B1 in vitro K_i values reported from literatures. Sensitivity analysis revealed that decreasing K_i for OATP1B1 improved predictions, indicating possible discrepancy between in vitro and “in vivo” K_i values for these two inhibitors. K_i values of inhibitor drugs on OATP1B1 need to be carefully evaluated with known substrates for a comprehensive DDI risk assessment. The under-predictions suggest that modeling drug transporter kinetics using PBPK requires further research to improve overall predictive performance for drug transporters.

Acknowledgements We thank Dr. Vicky Hsu for her critical review of this paper.

Compliance with ethical standards

Funding We thank the FDA Commissioner’s Fellowship Program that provided support to Dr. Peng Duan.

Conflict of interest Peng Duan, Ping Zhao and Lei Zhang have no conflict of interest.

References

1. Bjornstad P, Wadwa RP. Risks and benefits of statin use in young people with type 1 diabetes. *Curr Diab Rep.* 2014;14(7):499.
2. Botorff MB. Statin safety and drug interactions: clinical implications. *Am J Cardiol.* 2006;97(8A):27C–31C.
3. Egger SS, Ratz Bravo AE, Hess L, Schlienger RG, Krahenbuhl S. Age-related differences in the prevalence of potential drug-drug interactions in ambulatory dyslipidaemic patients treated with statins. *Drugs Aging.* 2007;24(5):429–40.
4. Neuvonen PJ, Niemi M, Backman JT. Drug interactions with lipid-lowering drugs: mechanisms and clinical relevance. *Clin Pharmacol Ther.* 2006;80(6):565–81.

5. Bellosta S, Corsini A. Statin drug interactions and related adverse reactions. *Expert Opin Drug Saf.* 2012;11(6):933–46.
6. Ho RH, Tirona RG, Leake BF, Glaeser H, Lee W, Lemke CJ, et al. Drug and bile acid transporters in rosuvastatin hepatic uptake: function, expression, and pharmacogenetics. *Gastroenterology.* 2006;130(6):1793–806.
7. Kopplow K, Letschert K, König J, Walter B, Keppler D. Human hepatobiliary transport of organic anions analyzed by quadruple-transfected cells. *Mol Pharmacol.* 2005;68(4):1031–8.
8. Kameyama Y, Yamashita K, Kobayashi K, Hosokawa M, Chiba K. Functional characterization of SLCO1B1 (OATP-C) variants, SLCO1B1*5, SLCO1B1*15 and SLCO1B1*15 + C1007G, by using transient expression systems of HeLa and HEK293 cells. *Pharmacogenet Genomics.* 2005;15(7):513–22.
9. Deng JW, Song IS, Shin HJ, Yeo CW, Cho DY, Shon JH, et al. The effect of SLCO1B1*15 on the disposition of pravastatin and pitavastatin is substrate dependent: the contribution of transporting activity changes by SLCO1B1*15. *Pharmacogenet Genomics.* 2008;18(5):424–33.
10. Tirona RG, Leake BF, Merino G, Kim RB. Polymorphisms in OATP-C: identification of multiple allelic variants associated with altered transport activity among European- and African-Americans. *J Biol Chem.* 2001;276(38):35669–75.
11. Li R, Barton HA, Maurer TS. Toward Prospective Prediction of Pharmacokinetics in OATP1B1 Genetic Variant Populations. *CPT Pharmacometr Syst Pharmacol.* 2014;3:e151.
12. Rose RH, Neuhoff S, Abduljalil K, Chetty M, Rostami-Hodjegan A, Jamei M. Application of a physiologically based pharmacokinetic model to predict OATP1B1-related variability in pharmacodynamics of rosuvastatin. *CPT Pharmacometr Syst Pharmacol.* 2014;3:e124.
13. Elsbey R, Hilgendorf C, Fenner K. Understanding the critical disposition pathways of statins to assess drug-drug interaction risk during drug development: it's not just about OATP1B1. *Clin Pharmacol Ther.* 2012;92(5):584–98.
14. Kwon Y, Morris ME. Membrane transport in hepatic clearance of drugs. I: Extended hepatic clearance models incorporating concentration-dependent transport and elimination processes. *Pharm Res.* 1997;14(6):774–9.
15. Duan P, Zhao P, Zhang L. Predicting statin-associated drug-drug interactions (DDIs) with static DDI models. In: Meeting abstract of 2013 Annual Meeting of American Association of Pharmaceutical Science (AAPS). 2013.
16. Zamek-Gliszczyński MJ, Lee CA, Poirier A, Bentz J, Chu X, Ellens H, et al. ITC recommendations for transporter kinetic parameter estimation and translational modeling of transport-mediated PK and DDIs in humans. *Clin Pharmacol Ther.* 2013;94(1):64–79.
17. Jones HM, Chen Y, Gibson C, Heimbach T, Parrott N, Peters SA, et al. Physiologically based pharmacokinetic modeling in drug discovery and development: a pharmaceutical industry perspective. *Clin Pharmacol Ther.* 2015;97(3):247–62.
18. Bosgra S, van de Steeg E, Vlaming ML, Verhoeckx KC, Huisman MT, Verwei M, et al. Predicting carrier-mediated hepatic disposition of rosuvastatin in man by scaling from individual transfected cell-lines in vitro using absolute transporter protein quantification and PBPK modeling. *Eur J Pharm Sci.* 2014;18(65):156–66.
19. Varma MV, Lai Y, Feng B, Litchfield J, Goosen TC, Bergman A. Physiologically based modeling of pravastatin transporter-mediated hepatobiliary disposition and drug-drug interactions. *Pharm Res.* 2012;29(10):2860–73.
20. Guidance for Industry: Drug interaction studies-study design, data analysis, implications for dosing, and labeling recommendation. 2012. USFDA. Silver Spring, MD, USA.
21. Jamei M, Bajot F, Neuhoff S, Barter Z, Yang J, Rostami-Hodjegan A, et al. A mechanistic framework for in vitro-in vivo extrapolation of liver membrane transporters: prediction of drug-drug interaction between rosuvastatin and cyclosporine. *Clin Pharmacokinet.* 2014;53(1):73–87.
22. Gertz M, Houston JB, Galetin A. Physiologically based pharmacokinetic modeling of intestinal first-pass metabolism of CYP3A substrates with high intestinal extraction. *Drug Metabol Dispos Biol Fate Chem.* 2011;39(9):1633–42.
23. Pitavastatin Clinical Pharmacology and Biopharmaceutics Review. <http://www.accessdata.fda.gov/scripts/cder/drugsatfda/index.cfm>. Accessed 12 Oct 2016.
24. Hirano M, Maeda K, Shitara Y, Sugiyama Y. Drug-drug interaction between pitavastatin and various drugs via OATP1B1. *Drug Metabol Dispos Biol Fate Chem.* 2006;34(7):1229–36.
25. Siedlik PH, Olson SC, Yang BB, Stern RH. Erythromycin coadministration increases plasma atorvastatin concentrations. *J Clin Pharmacol.* 1999;39(5):501–4.
26. Backman JT, Luurila H, Neuvonen M, Neuvonen PJ. Rifampin markedly decreases and gemfibrozil increases the plasma concentrations of atorvastatin and its metabolites. *Clin Pharmacol Ther.* 2005;78(2):154–67.
27. Lennernas H. Clinical pharmacokinetics of atorvastatin. *Clin Pharmacokinet.* 2003;42(13):1141–60.
28. Gertz M, Harrison A, Houston JB, Galetin A. Prediction of human intestinal first-pass metabolism of 25 CYP3A substrates from in vitro clearance and permeability data. *Drug Metabol Dispos Biol Fate Chem.* 2010;38(7):1147–58.
29. Soars MG, Grime K, Sproston JL, Webborn PJ, Riley RJ. Use of hepatocytes to assess the contribution of hepatic uptake to clearance in vivo. *Drug Metabol Dispos Biol Fate Chem.* 2007;35(6):859–65.
30. Pan HY, Willard DA, Funke PT, and McKinstry DN. The clinical pharmacology of SQ 31000 (CS-514) in healthy subjects. *Drugs Affect Lipid Metab.* 1987:255–9.
31. Jacobsen W, Kuhn B, Soldner A, Kirchner G, Sewing KF, Kollman PA, et al. Lactonization is the critical first step in the disposition of the 3-hydroxy-3-methylglutaryl-CoA reductase inhibitor atorvastatin. *Drug Metab Dispos.* 2000;28(11):1369–78.
32. Keskitalo JE, Zolk O, Fromm MF, Kurkinen KJ, Neuvonen PJ, Niemi M. ABCG2 polymorphism markedly affects the pharmacokinetics of atorvastatin and rosuvastatin. *Clin Pharmacol Ther.* 2009;86(2):197–203.
33. Posvar EL, Radulovic LL, Cilla DD Jr, Whitfield LR, Sedman AJ. Tolerance and pharmacokinetics of single-dose atorvastatin, a potent inhibitor of HMG-CoA reductase, in healthy subjects. *J Clin Pharmacol.* 1996;36(8):728–31.
34. Kimoto E, Walsky R, Zhang H, Bi YA, Whalen KM, Yang YS, et al. Differential modulation of cytochrome P450 activity and the effect of 1-aminobenzotriazole on hepatic transport in sandwich-cultured human hepatocytes. *Drug Metabol Dispos Biol Fate Chem.* 2012;40(2):407–11.
35. Derks M, Abt M, Parr G, Meneses-Lorente G, Young AM, Phelan M. No clinically relevant drug-drug interactions when dalcetapib is co-administered with atorvastatin. *Expert Opin Investig Drugs.* 2010;19(10):1135–45.
36. Rowland Yeo K, Walsky RL, Jamei M, Rostami-Hodjegan A, Tucker GT. Prediction of time-dependent CYP3A4 drug-drug interactions by physiologically based pharmacokinetic modelling: impact of inactivation parameters and enzyme turnover. *Eur J Pharm Sci.* 2011;43(3):160–73.
37. Varma MV, Lai Y, Kimoto E, Goosen TC, El-Kattan AF, Kumar V. Mechanistic modeling to predict the transporter- and enzyme-mediated drug-drug interactions of repaglinide. *Pharm Res.* 2013;30(4):1188–99.

38. Varma MV, Lin J, Bi YA, Rotter CJ, Fahmi OA, Lam JL, et al. Quantitative prediction of repaglinide-rifampicin complex drug interactions using dynamic and static mechanistic models: delineating differential CYP3A4 induction and OATP1B1 inhibition potential of rifampicin. *Drug Metabol Dispos Biol Fate Chem.* 2013;41(5):966–74.
39. Abduljalil K, Cain T, Humphries H, Rostami-Hodjegan A. Deciding on success criteria for predictability of pharmacokinetic parameters from *in vitro* studies: an analysis based on *in vivo* observations. *Drug Metabol Dispos Biol Fate Chem.* 2014;42(9):1478–84.
40. Sager JE, Yu J, Ragueneau-Majlessi I, Isoherranen N. Physiologically Based Pharmacokinetic (PBPK) Modeling and Simulation Approaches: A Systematic Review of Published Models, Applications, and Model Verification. *Drug Metab Dispos.* 2015;43(11):1823–37.
41. Sager JE, Lutz JD, Foti RS, Davis C, Kunze KL, Isoherranen N. Fluoxetine- and norfluoxetine-mediated complex drug-drug interactions: *in vitro* to *in vivo* correlation of effects on CYP2D6, CYP2C19, and CYP3A4. *Clin Pharmacol Ther.* 2014;95(6):653–62.
42. Chetty M, Li L, Rose R, Machavaram K, Jamei M, Rostami-Hodjegan A, et al. Prediction of the Pharmacokinetics, Pharmacodynamics, and Efficacy of a Monoclonal Antibody, Using a Physiologically Based Pharmacokinetic FcRn Model. *Front Immunol.* 2014;5:670.
43. Asberg A, Hartmann A, Fjeldsa E, Bergan S, Holdaas H. Bilateral pharmacokinetic interaction between cyclosporine A and atorvastatin in renal transplant recipients. *Am J Transpl.* 2001;1(4):382–6.
44. Amundsen R, Christensen H, Zabihyan B, Asberg A. Cyclosporine A, but not tacrolimus, shows relevant inhibition of organic anion-transporting protein 1B1-mediated transport of atorvastatin. *Drug Metabol Dispos Biol Fate Chem.* 2010;38(9):1499–504.
45. Harwood MD, Neuhoff S, Carlson GL, Warhurst G, Rostami-Hodjegan A. Absolute abundance and function of intestinal drug transporters: a prerequisite for fully mechanistic *in vitro*-*in vivo* extrapolation of oral drug absorption. *Biopharm Drug Dispos.* 2013;34(1):2–28.
46. Jones HM, Barton HA, Lai Y, Bi YA, Kimoto E, Kempshall S, et al. Mechanistic pharmacokinetic modeling for the prediction of transporter-mediated disposition in humans from sandwich culture human hepatocyte data. *Drug Metabol Dispos Biol Fate Chem.* 2012;40(5):1007–17.
47. Ieiri I, Suwannakul S, Maeda K, Uchamaru H, Hashimoto K, Kimura M, et al. SLCO1B1 (OATP1B1, an uptake transporter) and ABCG2 (BCRP, an efflux transporter) variant alleles and pharmacokinetics of pitavastatin in healthy volunteers. *Clin Pharmacol Ther.* 2007;82(5):541–7.
48. Pasanen MK, Fredrikson H, Neuvonen PJ, Niemi M. Different effects of SLCO1B1 polymorphism on the pharmacokinetics of atorvastatin and rosuvastatin. *Clin Pharmacol Ther.* 2007;82(6):726–33.
49. Maeda K, Ikeda Y, Fujita T, Yoshida K, Azuma Y, Haruyama Y, et al. Identification of the rate-determining process in the hepatic clearance of atorvastatin in a clinical cassette microdosing study. *Clin Pharmacol Ther.* 2011;90(4):575–81.
50. Snoeys J, Beumont M, Monshouwer M, Ouwerkerk-Mahadevan S. Mechanistic understanding of the nonlinear pharmacokinetics and intersubject variability of simeprevir: a PBPK-guided drug development approach. *Clin Pharmacol Ther.* 2016;99(2):224–34.
51. Venkataramanan R, Habucky K, Burckart GJ, Ptachcinski RJ. Clinical pharmacokinetics in organ transplant patients. *Clin Pharmacokinet.* 1989;16(3):134–61.
52. Martinez-Guerrero LJ, Wright SH. Substrate-dependent inhibition of human MATE1 by cationic ionic liquids. *J Pharmacol Exp Ther.* 2013;346(3):495–503.
53. Belzer M, Morales M, Jagadish B, Mash EA, Wright SH. Substrate-dependent ligand inhibition of the human organic cation transporter OCT2. *J Pharmacol Exp Ther.* 2013;346(2):300–10.
54. Izumi S, Nozaki Y, Komori T, Maeda K, Takenaka O, Kusano K, et al. Substrate-dependent inhibition of organic anion transporting polypeptide 1B1: comparative analysis with prototypical probe substrates estradiol-17 β -glucuronide, estrone-3-sulfate, and sulfobromophthalein. *Drug Metabol Dispos Biol Fate Chem.* 2013;41(10):1859–66.
55. Shitara Y, Takeuchi K, Horie T. Long-lasting inhibitory effects of saquinavir and ritonavir on OATP1B1-mediated uptake. *J Pharm Sci.* 2013;102(9):3427–35.
56. Kato M, Shitara Y, Sato H, Yoshisue K, Hirano M, Ikeda T, et al. The quantitative prediction of CYP-mediated drug interaction by physiologically based pharmacokinetic modeling. *Pharm Res.* 2008;25(8):1891–901.
57. Burt HJ, Neuhoff S, Almond L, Gaohua L, Harwood MD, Jamei M, et al. Metformin and cimetidine: physiologically based pharmacokinetic modelling to investigate transporter mediated drug-drug interactions. *Eur J Pharm Sci.* 2016;10(88):70–82.
58. Hsu V, de LTVM, Zhao P, Zhang L, Zheng JH, Nordmark A, et al. Towards quantitation of the effects of renal impairment and probenecid inhibition on kidney uptake and efflux transporters, using physiologically based pharmacokinetic modelling and simulations. *Clin Pharmacokinet.* 2014;53(3):283–93.
59. Pubchem. Pitavastatin compound. <https://pubchem.ncbi.nlm.nih.gov/compound/5282452>. Accessed Jan 2015.
60. Pubchem. Atorvastatin compound. <https://pubchem.ncbi.nlm.nih.gov/compound/60823>. Accessed Jan 2015.
61. ChemAxon. Pitavastatin compound.
62. ChemAxon. Atorvastatin compound.
63. Clinical Pharmacology and Biopharmaceutics Review of Atorvastatin. In: Pharmacology C, editor. Silver Spring: FDA; 1996.
64. Watanabe T, Kusuhara H, Maeda K, Kanamaru H, Saito Y, Hu Z, et al. Investigation of the rate-determining process in the hepatic elimination of HMG-CoA reductase inhibitors in rats and humans. *Drug Metabol Dispos Biol Fate Chem.* 2010;38(2):215–22.
65. Jamei M, Turner D, Yang J, Neuhoff S, Polak S, Rostami-Hodjegan A, et al. Population-based mechanistic prediction of oral drug absorption. *AAPS J.* 2009;11(2):225–37.
66. Wu X, Whitfield LR, Stewart BH. Atorvastatin transport in the Caco-2 cell model: contributions of P-glycoprotein and the proton-monocarboxylic acid co-transporter. *Pharm Res.* 2000;17(2):209–15.
67. Rodgers T, Leahy D, Rowland M. Physiologically based pharmacokinetic modeling 1: predicting the tissue distribution of moderate-to-strong bases. *J Pharm Sci.* 2005;94(6):1259–76.
68. Rodgers T, Rowland M. Physiologically based pharmacokinetic modelling 2: predicting the tissue distribution of acids, very weak bases, neutrals and zwitterions. *J Pharm Sci.* 2006;95(6):1238–57.
69. Rodgers T, Leahy D, Rowland M. Tissue distribution of basic drugs: accounting for enantiomeric, compound and regional differences amongst beta-blocking drugs in rat. *J Pharm Sci.* 2005;94(6):1237–48.
70. Rodgers T, Rowland M. Mechanistic approaches to volume of distribution predictions: understanding the processes. *Pharm Res.* 2007;24(5):918–33.
71. Vieira ML, Zhao P, Berglund EG, Reynolds KS, Zhang L, Lesko LJ, et al. Predicting drug interaction potential with a physiologically based pharmacokinetic model: a case study of telithromycin, a time-dependent CYP3A inhibitor. *Clin Pharmacol Ther.* 2012;91(4):700–8.

72. Fujino H, Yamada I, Shimada S, Yoneda M, Kojima J. Metabolic fate of pitavastatin, a new inhibitor of HMG-CoA reductase: human UDP-glucuronosyltransferase enzymes involved in lactonization. *Xenobiotica*. 2003;33(1):27–41.
73. Fujino H, Saito T, Tsunenari Y, Kojima J. Effect of gemfibrozil on the metabolism of pitavastatin—determining the best animal model for human CYP and UGT activities. *Drug Metab Drug Interact*. 2004;20(1–2):25–42.
74. Paine SW, Parker AJ, Gardiner P, Webborn PJ, Riley RJ. Prediction of the pharmacokinetics of atorvastatin, cerivastatin, and indomethacin using kinetic models applied to isolated rat hepatocytes. *Drug Metabol Dispos Biol Fate Chem*. 2008;36(7):1365–74.
75. De Bruyn T, van Westen GJ, Ijzerman AP, Stieger B, de Witte P, Augustijns PF, et al. Structure-based identification of OATP1B1/3 inhibitors. *Mol Pharmacol*. 2013;83(6):1257–67.
76. Foti RS, Rock DA, Wienkers LC, Wahlstrom JL. Selection of alternative CYP3A4 probe substrates for clinical drug interaction studies using in vitro data and in vivo simulation. *Drug Metabol Dispos Biol Fate Chem*. 2010;38(6):981–7.
77. Prueksaritanont T, Chu X, Evers R, Klopfer SO, Caro L, Kothare PA, et al. Pitavastatin is a more sensitive and selective organic anion-transporting polypeptide 1B clinical probe than rosuvastatin. *Br J Clin Pharmacol*. 2014;78(3):587–98.
78. Mazzu AL, Lasseter KC, Shamblen EC, Agarwal V, Lettieri J, Sundaresen P. Itraconazole alters the pharmacokinetics of atorvastatin to a greater extent than either cerivastatin or pravastatin. *Clin Pharmacol Ther*. 2000;68(4):391–400.
79. Lau YY, Huang Y, Frassetto L, Benet LZ. effect of OATP1B transporter inhibition on the pharmacokinetics of atorvastatin in healthy volunteers. *Clin Pharmacol Ther*. 2007;81(2):194–204.
80. Chen Y, Zhang W, Huang WH, Tan ZR, Wang YC, Huang X, et al. Effect of a single-dose rifampin on the pharmacokinetics of pitavastatin in healthy volunteers. *Eur J Clin Pharmacol*. 2013;69(11):1933–8.
81. Whitfield LR, Porcari AR, Alvey C, Abel R, Bullen W, Hartman D. Effect of gemfibrozil and fenofibrate on the pharmacokinetics of atorvastatin. *J Clin Pharmacol*. 2011;51(3):378–88.